Endocytic Vesicles from Renal Papilla Which Retrieve the Vasopressin-sensitive Water Channel Do Not Contain a Functional H+ATPase

Wayne I. Lencer,* A. S. Verkman,‡ M. Amin Arnaout, Dennis A. Ausiello, and Dennis Brown

Renal Unit and * Combined Program in Pediatric Gastroenterology and Nutrition, Massachusetts General Hospital; and Departments of Medicine, Pediatrics, and Pathology, Harvard Medical School, Boston, Massachusetts 02114; and ‡ Department of Medicine and Cardiovascular Research Institute, University of California, San Francisco, California 94143

Abstract. The water permeability of the kidney collecting duct epithelium is regulated by vasopressin (VP)-induced recycling of water channels between an intracellular vesicular compartment and the plasma membrane of principal cells. To test whether the water channels pass through an acidic endosomal compartment during the endocytic portion of this pathway, we measured ATP-dependent acidification of FITC-dextran–labeled endosomes in isolated microsomal fractions from different regions of Brattleboro rat kidneys. Both VP-deficient controls and rats treated with exogenous VP were examined. ATP-dependent acidification was not detectable in endosomes containing water channels from distal papilla (osmotic water permeability P_f = 0.038 ± 0.004 cm/s). In contrast, the addition of ATP resulted in a strong acidification of renal cortical endosomes (pH_{min} = 5.8, initial rate = 0.18 − 0.25 pH U/s). Acidification of cortical endosomes was reversed with nigericin and strongly inhibited by N-ethyl-maleimide. Passive proton permeability was similar and low in both cortical and papillary endosomes from rats treated or not treated with VP. The fraction of labeled endosomes present in microsomal preparations was determined by fluorescence imaging microscopy of microsomes nonspecifically bound to poly-1-lysine–coated coverslips and was 25% in cortical preparations compared to 14% (+VP) and 9% (−VP) in papillary preparations. The fraction of cortical endosomes was enriched 1.5-fold by immunoabsorption to coverslips coated with mAbs against the bovine vacuolar proton pump. In contrast, the fraction of papillary endosomes was depleted more than twofold by immunoabsorption to identical coverslips. Finally, sections of distal papilla stained with antibodies against the lysosomal glycoprotein LGP120 showed that most of the entrapped FITC-dextran did not colocalize with this lysosomal protein. These results demonstrate that vesicles which internalize water channels in kidney collecting duct principal cells lack functional proton pumps, and do not deliver the bulk of their FITC-dextran content to lysosomes. The data suggest that the principal cell contains a specialized nonacidic apical endocytic compartment which functions primarily to recycle membrane components, including water channels, to the plasma membrane.

I N mammalian cells, endocytic vesicles usually fuse with an acidic intracellular compartment where receptor/ligand dissociation occurs. In this endosomal compartment, internalized proteins are sorted and either targeted back to the plasma membrane or into a lysosomal degradative pathway (12, 26). The cellular mechanism responsible for the regulation of water reabsorption in the collecting duct of the mammalian kidney is also thought to involve a cycle of exo- and endocytosis during which specialized vesicles, whose limiting membranes contain water channels, are shuttled between the apical plasma membrane and the apical cytoplasm of principal cells (4, 9, 20, 42). We demonstrated recently that vasopressin (VP)[1] induces the endocytosis of

functional water channels from the apical membrane of collecting duct principal cells, and that the presence of water channels in the limiting membrane of endosomes from these cells correlated with the antidiuretic state of the rat before kidney removal (43; Lencer, W. I., D. Brown, D. A. Ausiello, and A. S. Verkman, manuscript submitted for publication). It is not known, however, whether internalized water channels in the mammalian kidney undergo further processing in an acidic intracellular compartment, or whether they recycle to the apical membrane in response to repeated stimulation by VP.

To determine whether water channels retrieved from the apical membrane of principal cells after VP stimulation enter an acidic prelysosomal compartment, we infused the membrane impermeant fluorophores, 6-carboxyfluorescein (6-CF) and FITC-dextran into Brattleboro rats as previously

---

1. *Abbreviations used in this paper:* 6-CF, 6-carboxyfluorescein; VP, vasopressin.

described (43). The Brattleboro rat is congenitally deficient in VP (38), but has a normal renal response to exogenous VP. The fluorophores were filtered in the kidney glomerulus and appeared rapidly in the tubule lumen where they were available as fluid phase markers of endocytosis. Taking advantage of the rapid response (<< 1 ms) of the fluorescein tracer to changes in vesicle volume or pH, direct measurements of endosome water and proton transport were made on the selective population of fluorescein-labeled endocytic vesicles in crude microsomal preparations. The water permeability and proton transport of unlabeled vesicles (i.e., nonendocytic) which were also present in the microsomal fractions were not measured in these fluorescence quenching assays.

Our results demonstrate that 15 and 30 min after endocytic retrieval of water channels in collecting duct principal cells, VP-induced endosomes which internalize apical membrane water channels do not contain a functional H⁺ATPase in their limiting membrane. In addition, these vesicles do not deliver appreciable amounts of FITC-dextran to lysosomes. The data suggest that regulation of water permeability in the apical membrane of collecting duct principal cells involves endocytic vesicles which are dedicated to return to the apical membrane without passage through an acidic prelysosomal compartment.

Materials and Methods

Materials

mAbs to the vacuolar proton pump were obtained from Steve Gluck (Washington University, St. Louis, MO) and polyclonal antibodies to lysosomal protein LGP-120 from Ira Mellman (Yale University, New Haven, CT). Inactin was purchased from Byk Gulden (Konstanz, W. Germany), and polylysine from Polysciences, Inc. (Warrington, PA). Rhodamine-labeled goat anti–rabbit IgG was obtained from Boehringer Mannheim Biochemicals (Indianapolis, IN). All other reagents were purchased from Sigma Chemical Co. (St. Louis, MO). 6-CF was dissolved in PBS (150 mM NaCl, 10 mM Na phosphate, pH 7.4) at a concentration of 7.5 mM or 15 mM and filtered. FITC-dextran (10,000 D) was dissolved in PBS at a concentration of 25 mg/ml and dialyzed against two 1-liter vol of PBS for a total of 48 h to remove unbound fluorescein. Antifluorescein antibody was raised in rabbits immunized with FITC-conjugated ovalbumin or keyhole limpet hemocyanin as described by Sklar et al. (34).

Labeling of Endosomes from Rat Kidney

Brattleboro rats, dehydrated for 12–18 h, were anesthetized with Inactin (13–16 mg/100 g body weight, i.p.), tracheotomized, and maintained at 37°C on a heating pad. 6-CF (7.5 mg/ml) or FITC-dextran (25 mg/ml) with or without VP (2.5 μg/ml) was injected as a bolus (1 ml/100 g wt) into the jugular vein of Brattleboro rats over 1 min. After 15 or 30 min, the inferior vena cava was cut and the rats were perfused through the left ventricle with buffer A (50 mM mannitol, 5 mM Na phosphate, pH 8.5) until the kidneys blanched (~1 min) for water transport studies, or with HBSS (118 mM NaCl, 4.7 mM KCl, 1.25 mM CaCl₂, 1.2 mM MgSO₄, 1.2 mM KH₂PO₄, 25 mM NaHCO₃) for proton transport studies. The kidneys were excised and placed in cold buffer. All subsequent steps were carried out at 4°C. Kidneys were opened at the uretero–pelvic junction and cut sagitally to expose the intact inner medulla and sections of inner stripe, outer stripe, and cortex. Thin superficial shavings (~1 mm) of cortex were removed, and the inner medulla below the inner stripe was dissected and divided into proximal and distal sections. We defined distal papilla as the lower portion of the inner medulla that was not adherent to surrounding inner stripe. Finally, tissue from the inner stripe was dissected distal to the visible junction between inner and outer stripe. Light micrographs of inner stripe proximal to the dissected sections removed for homogenization showed that proximal tubules were absent (data not shown). Tissue was homogenized in buffer A

for water transport studies or in buffer B (50 mM KCl, 10 mM K phosphate, 1 mM MgCl₂, 1 μM PMSF, pH 7.5) for proton transport studies by 15 gentle strokes in a Potter-Elvehjem homogenizer and centrifuged at 500 g for 10 min; the supernatant was recentrifuged at 5,000 g for an additional 10 min. The resulting supernatant was centrifuged at 100,000 g for 1 h to yield a microsomal pellet which contained endosomes labeled with entrapped 6-CF or FITC-dextran. The pellet was washed once in 100 vol of buffer A or B and the final microsomal pellet was homogenized in 1 ml of buffer A or B by aspirating the sample through 23- and 27-gauge steel needles, yielding 0.10-0.17 mg membrane protein/kidney for papillary samples and 0.55-0.60 mg membrane protein/kidney for cortical samples. We quantified the distribution of intravesicular fluorescence throughout the preparation procedure and found that the final pellet assayed contained 12–25% of the total intravesicular fluorescence present in the initial cellular homogenate depending on the kidney region examined, and 43–73% of the intravesicular fluorescence present in the supernatant from the first low-speed spin (i.e., after all intact cells and residual tissue fragments had been spun down). When kept at 4°C the leakage of FITC-dextran from labeled endosomes isolated from each region of the kidney was 0.2-0.4%/h over 72 h. Greater than 85% of the internalized FITC-dextran remained in vesicles from the papilla 72 h after preparation. Leakage of FITC-dextran was also measured in vesicles exposed to either a 100-mosM sucrose gradient or to an equal volume of isosmotic buffer in an SLM fluorimeter (to document water efflux). The vesicles were pelleted after exposure to the different buffers and the fluorescein intensity of the supernatant was measured. There was an identical and minimal leakage in both cases. Total fluorescence (F) in supernatant was 45.08 ± 0.047 F/mg protein/h for control vesicles and 45.03 ± 0.047 F/mg protein/h for sucrose-treated vesicles or ~2.9% leakage over 1 h at 37°C in both cases.

Osmotic Water Permeability in Endosomes

Osmotic water permeability was measured by a stopped-flow fluorescence quenching technique (32, 46). Suspensions of the microsomal pellet (0.05-0.08 mg protein/ml for papilla and 0.55-0.6 mg protein/ml for cortex) in buffer A were subject to a 100-mM inwardly directed osmotic (sucrose) gradient in a stopped-flow apparatus (Hi-Tech SF51; Wiltshire, England). The instrument dead time was 1.7 ms. The sample was excited at 465 ± 5 nm by a monochromator in series with a 420-490-nm interference filter (Omega Optical, Brattleboro, VT). Fluorescence was detected through a 515-nm cut-on filter (Schott Glass, Duryea, PA). Experiments were performed at 21°C. Data were acquired at a maximal rate of 0.2 ms/point. Four to six measurements of water permeability were performed on every sample for signal averaging.

Fluorescence kinetic data (512 points/experiment) were fitted to single or double exponential functions by a nonlinear regression procedure. Osmotic water permeability coefficients (P_f) were calculated from exponential time constants and endocytic vesicle geometry as described previously (10). An endocytic vesicle surface-to-volume ratio of 3.3×10^5 cm⁻¹ was used based on the measured mean vesicle diameter of 183 ± 7 nm.

ATP-dependent Proton Transport in Endosomes

ATP-driven proton transport was measured in endosomes labeled with FITC-dextran by making use of the pH sensitivity of FITC-dextran (46). Microsomes (~20 μg protein/ml) were added to 2 ml of buffer B in an acrylic cuvette maintained at 37°C. The microsomes were "voltage clamped" with 1 μM valinomycin and freshly prepared ATP (500 mM stock, pH 7.5) was added to give a final concentration of 1 mM. Fluorescence was excited at 490 nm in a fluorimeter (model 8000; SLM, Urbana, IL) and the emission was filtered by two 515-nm cut-on filters (Schott Glass) in series. Data were averaged over 1-s intervals. After endosome pH stabilized, 1 μM nigericin (stock 1 mM) was added to collapse the pH gradient. To determine the relation between fluorescence and intravesicular pH, the fluorescent signal arising from extravesicular FITC-dextran was determined by adding successive aliquots of a polyclonal antifluorescein antibody until no further fluorescence quenching was observed. To determine the baseline signal at the end of each experiment, 50 μl of 1 M HCl was added to quench the fluorescein signal completely. The difference between the sum of the extravesicular and baseline fluorescence from the total fluorescent signal gave a quantitative measure of intravesicular fluorescence. Absolute pH values were calculated from fluorescence intensities, the fraction of intravesicular FITC-fluorescence, and the calibration between fluorescence and pH as described by Ye et al. (46).

Passive Proton Permeability in Endosomes

Passive proton permeability was measured in endosomes labeled with FITC-dextran from the time course of fluorescence in response to a 1.5-pH U inward proton gradient (41). Microsomes containing 50 mM KCl buffer at pH 7.5 and the potassium ionophore valinomycin (2 μl of 1 mM stock) were mixed in the stopped-flow apparatus with an equal volume of 50 mM KCl buffer titrated with HCl so that when mixed, the final external pH was 6.0. Fluorescence was excited at 480 $\pm$ 5 nm and measured at >520 nm. The initial proton flux (J_H; meq H$^+$/L/s) was determined from the initial rate of fluorescence decrease ($dF(0)/dt$; fluorescence units/s), the intravesicular buffer capacity (B(pH); meq OH$^-$/L/pH U), the normalized pH vs. fluorescein-dextran fluorescence (f) calibration relation (above), and the fluorescence intensities at pH 7.5 and 6.0 ($F_{7.5}$ and $F_{6.0}$) by the relation (33),

$$ J_H = \frac{dF(0)}{dt} \, B \, (\text{pH}) \left[\frac{f_{7.5} - f_{6.0}}{F_{7.5} - F_{6.0}} \right] $$

$dF(0)/dt$ was determined from the initial slope of an exponential fitted to the first 2 s of the fluorescence time course. B(pH) was determined by the magnitude of the pH decrease in response to a 15-mM inward gradient of formic acid, a weak acid in which the protonated moiety permeates rapidly and undergoes almost complete dissociation within the endosome. d(pH)/dF was determined from the calibration relation to be 4.3 pH U at pH 7.5. The two calibration points, $F_{7.5}$ and $F_{6.0}$, were determined by subjecting microsomes to a 1.5-pH U inward proton gradient in the presence of the K$^+$/H$^+$ exchanger nigericin (5 μM). In the presence of nigericin, intravesicular pH rapidly equilibrates with the external pH. The fluorescence at the start of the data trace was $F_{7.5}$; the fluorescence intensity after pH equilibration was $F_{6.0}$. The two calibration points were required to provide an absolute pH scale for fluorescence intensities measured in the stopped-flow apparatus. The factor $f_{7.5}$-$f_{6.0}$ was determined from the calibration relation to be 0.62. The proton permeability coefficient (P$_H$ in cm/s) was calculated from the ratio $J_H/([\Delta H^+]*S/V)$, where S/V is endosome surface-to-volume ratio.

Visualization of FITC-labeled Endosomes in Tissue Sections

To localize endosomes labeled with FITC-dextran in tissue sections, Brattleboro rats were infused with FITC-dextran (25 mg/ml) $\pm$ VP (2.5 μg/ml) as described above. After 15 or 30 min, the rats were perfused through the left ventricle with HBSS until the kidneys blanched (usually ~1 min), and the tissue was fixed by continued perfusion with 2% paraformaldehyde, 75 mM lysine, and 10 mM periodate (25). After perfusion fixation until the kidneys hardened (5–10 min), tissues were removed, cut into smaller pieces, and fixed further in PLP by immersion overnight at 4°C.

Endosomes containing entrapped FITC-dextran were visualized in intact tissue by fluorescence microscopy as described recently (21). Small pieces of fixed papilla were washed extensively in PBS and immersed in 2.3 M sucrose in PBS for at least 1 h. Tissue was frozen by immersion in liquid nitrogen or in Freon 22 cooled with liquid nitrogen. Semi-thin sections (1 μm) were cut on a Reichert FC4 ultracryomicrotome (Donsanto Corp., Natick, MA), collected on glass slides, and coverslipped using a drop of 50% PBS/50% glycerol containing 4% n-propyl-gallate to retard fading (16). Some sections were also immunostained to reveal the lysosomal glycoprotein LGP120 (see below). The sections were examined using a Nikon FXA photomicroscope (Donsanto Corp., Natick, MA), equipped with a 480 $\pm$ 10-nm excitation filter and a 520 $\pm$ 20-nm barrier filter for fluorescein label, and 546 $\pm$ 5-nm excitation filter and a 580-nm barrier filter for rhodamine fluorescence. Photographs were taken using Tri-X Pan or T-Max 400 film (Eastman Kodak Co., Rochester, NY).

Immunocytochemistry

Semi-thin (1 μm) cryostat sections on glass slides were incubated for 10 min with PBS containing 1% BSA. 20 μl of anti-LGP120 diluted 1:50 in PBS/albumin was then applied to tissue sections and incubated at room temperature for 1 h. The sections were rinsed three times with PBS/albumin (5 min each) and incubated for 1 h at room temperature with a 1:100 dilution of a rhodamine-labeled goat anti-rabbit IgG antibody (15 μg/ml final concentration). The sections were rinsed again in PBS, coverslipped using a drop of PBS/glycerol containing 4% n-propyl-gallate, and visualized as described above.

Immunoabsorption of Endosomes and Fluorescence Imaging

For immunoabsorption studies, endosomes were labeled with rhodamine dextran (RITC-dextran; 10 kD) by perfusing rats with 25 mg/100 g wt RITC-dextran in place of FITC-dextran. Microsomal preparations of cortex and papilla were prepared as described above. To label nonendocytic vesicles with 6-CF and double label endosomes (which already contained entrapped RITC-dextran) with 6-CF, microsomal pellets were incubated for 36 h at 4°C with buffer B containing 2.5 mM 6-CF at pH 6.0. After equilibration, 6-CF was trapped inside these vesicles by raising buffer pH to 8.0. The vesicles were washed by centrifugation to remove 6-CF in solution.

Clean glass coverslips were coated with either 0.01 mg/ml polylysine or monoclonal antiproton pump antibody (47) (1.5 mg/ml) diluted 1:100 in PBS. This antibody recognizes a cytoplasmic epitope of kidney vacuolar H$^+$ATPase, and has been used for the affinity purification of proton pumps in previous studies (18). Coverslips were then washed with three changes of PBS or PBS/1% albumin, respectively. 6-CF-labeled microsomes (~20 μg protein/ml) were then applied to either polylysine or anti-H$^+$ATPase antibody–coated coverslips for 30 min at room temperature. The coverslips were then washed with three changes of PBS/1% albumin for 5 min each and mounted on glass slides with a drop of PBS. Nonendocytic vesicles, containing only 6-CF, and endosomes, containing both RITC-dextran and 6-CF, which bound to the coverslip surface, were excited with a 100-W mercury arc lamp in a Nikon FXA photomicroscope equipped with a 100× oil immersion objective (NA 1.4). The vesicles were visualized using an image intensifier (Videoscope, Dulles International Airport, Dallas, TX) in series with a Dage-MTI SIT camera (Michigan City, IN) interfaced to a SMI digitizer (Atlanta, GA), Poynting averaging box (Oak Park, IL), and IBM-compatible computer. 6-CF fluorescence was excited at 480 $\pm$ 10 nm and measured at 520 $\pm$ 20 nm. Rhodamine fluorescence was excited at 546 $\pm$ 5 nm and measured at >580 nm by a cut-on filter. Photographs of fluorescein and rhodamine images (average of 256 successive frames) of the same field were taken directly from the video monitor and used to quantitate the proportion of endosomes (vesicles containing both 6-CF and RITC-dextran) absorbed onto either poly-l-lysine or proton pump antibody–coated coverslips.

Results

Localization of FITC-Dextran in Semi-thin Sections

The fluorescence micrographs in Fig. 1 show that the distal papilla contains fluorescein-labeled endosomes specific to principal cells (Fig. 1, a and b), whereas both principal and intercalated cells are present in the proximal papilla and they both contain fluorescein-labeled endosomes (Fig. 1 d). Intercalated cells internalized more FITC-dextran than neighboring principal cells in both VP-treated and untreated rats. Micrographs of inner stripe also show FITC-dextran uptake into both intercalated and principal cells of the collecting duct as well as into epithelia lining thick ascending limbs (data not shown). Intercalated cells were present in greater numbers in collecting ducts of inner stripe compared to proximal papilla. 15 min after VP and FITC-dextran infusion, the fluorescein-labeled endosomes in the distal papilla were concentrated beneath the apical membrane of principal cells. Other cell types in the papilla, such as epithelial cells of thin limbs of Henle and capillary endothelial cells, did not internalize detectable amounts of FITC-dextran. Principal cells from animals pretreated with VP (Fig. 1 a) internalized more FITC-dextran than principal cells from untreated animals (Fig. 1 b).

Measurement of Active Proton Transport in Endosomes

15 min after FITC-dextran infusion, endosomes prepared from the renal papilla (combined proximal and distal re-
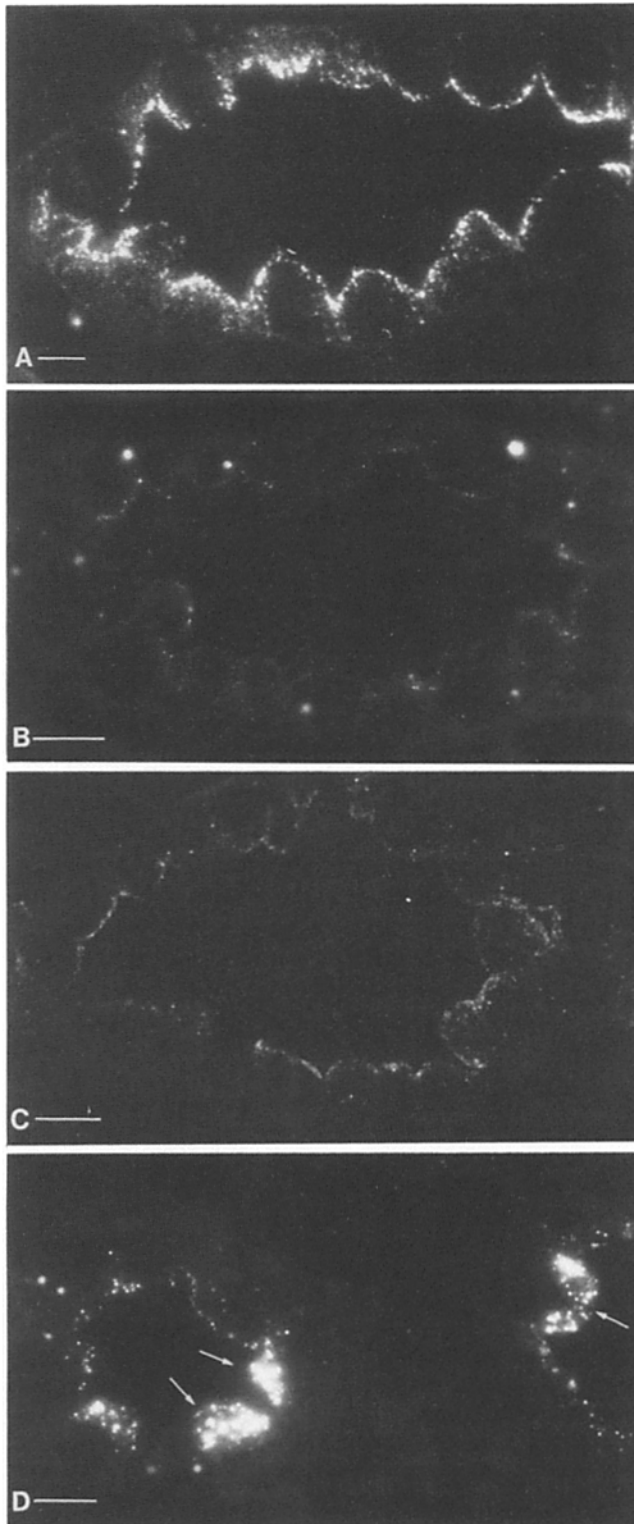
Figure 2. ATP-dependent acidification of endosomes from the cortex and papilla of Brattleboro rats treated (+VP) and not treated (−VP) with VP. Endosomes labeled with FITC-dextran in buffer B were "voltage clamped" with valinomycin (VAL) and exposed to 1 mM ATP at 37°C. After endosome pH stabilized, nigericin (NIG) was added to collapse the proton gradient and return the fluorescent signal to baseline. The signal was corrected to account for extravesicular FITC-dextran by the addition of successive aliquots of polyclonal antifluorescein antibody (Ab). HCl was then added to quench the fluorescent signal completely and give a two-point calibration which was used to quantitate endosomal pH (see Materials and Methods). Curves were individually normalized to the same pH scale.

gions) of rats treated or not treated with VP acidified much less than endosomes prepared from the renal cortex of the same kidneys (Fig. 2 and mean ± SEM, n = 3: cortex ± VP: 5.65 ± 0.35; papilla + VP: 7.37 ± 0.05; papilla − VP: 7.26 ± 0.06). The data indicate that the bulk of FITC-labeled endosomes from renal papilla did not contain a functional ATP-dependent proton pump. However, since endosomes from intercalated cells were also present in these microsomal fractions, we could not attribute the acidification properties of these vesicles to specific cell types in the collecting duct.

To examine proton (and water) transport in endosomes specific to principal cells, therefore, microsomal fractions from distal and proximal papilla and inner stripe (± VP) were examined. Fluorescein-labeled endosomes from renal cortex, which are derived mainly from the vasopressin-insensitive proximal tubule, served as controls. 15 min after FITC-dextran infusion, endosomes from renal cortex (Fig. 3 a), inner stripe (Fig. 3 b), and proximal papilla (Fig. 3 c) acidified in response to ATP, whereas endosomes from distal papilla (Fig. 3 d) did not (see Table I, 15 min). Furthermore,

Figure 1. Fluorescent micrographs of collecting ducts from the distal papilla of Brattleboro rats 15 min after infusion with FITC-dextran and VP (A) or FITC-dextran alone (B). Intercalated cells are not present in collecting ducts from this region of the kidney and the entire population of fluorescein-labeled endosomes originates specifically from principal cells. FITC-dextran did not label any other cell types in either the distal or proximal papilla. 15 min after FITC-dextran infusion, labeled endosomes from cells treated and not treated with VP were concentrated beneath the apical membrane. Uptake of FITC-dextran was greater in principal cells from
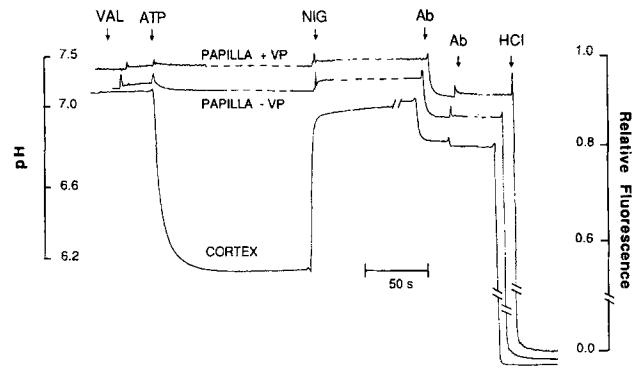
rats treated with VP (A) compared to principal cells from rats not treated with VP (B). Fluorescent micrograph (C) of a collecting duct from the distal papilla of a rat 30 min after infusion with FITC-dextran and VP shows that labeled endosomes remain concentrated beneath the apical membrane of principal cells but the density of labeled endosomes appears lower. Fluorescent micrograph (D) of a collecting duct from the proximal papilla 15 min after infusion with FITC-dextran and VP shows that both principal cells and intercalated cells (arrows) are present in collecting ducts and both cell types contain FITC-labeled endosomes. Intercalated cells contain more internalized FITC-dextran than principal cells whether or not the rats were treated with VP. Bars, 10 μm.
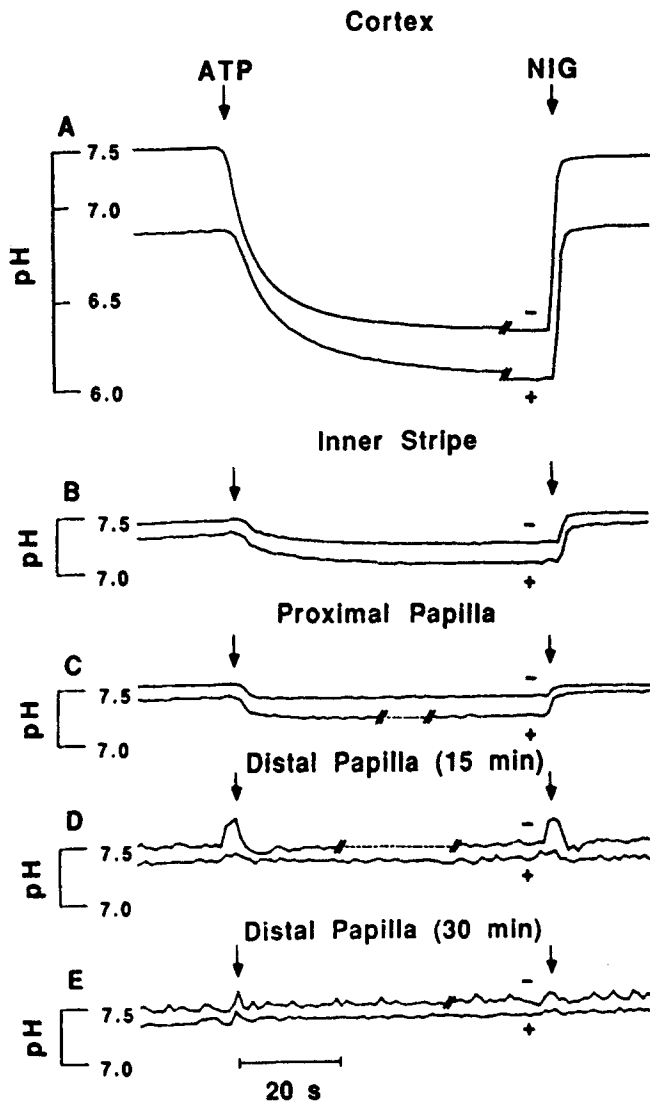
Figure 3. ATP-dependent acidification of endosomes from the cortex, inner stripe, proximal papilla, and distal papilla of Brattleboro rats treated (+) and not treated (−) with VP. Endosomes labeled with FITC-dextran in buffer B were examined for proton transport as described in Fig. 2. Curves were individually normalized to the same pH scale. Initial rates of proton transport and final pH are given in Table I.

we also examined the intermediate speed (5,000 g) pellet of our preparations for ATP-dependent proton transport and found that while acidification could be measured in this fraction from the cortex, the inner stripe, and the proximal papilla, no acidification was detectable in the distal papilla (data not shown). This indicates that we do not preferentially lose endosomes capable of acidification during the isolation procedure. ATP-dependent acidification of endosomes from cortex, inner stripe, and proximal papilla was not significantly affected by 500 μM vanadate and 10 μg/ml oligomycin, but was strongly inhibited (>95%) by 1 mM N-ethyl-maleimide. These sensitivities are characteristic of the vacuolar H$^+$AT-Pase described in cortical endosomes (46) and lysosomes (26, 28).

To test whether FITC-labeled endosomes from distal papilla might acidify after longer periods of incubation, we

examined proton transport in endosomes prepared from tissue 30 min after infusion of FITC-dextran ± VP (Table I, 30 min). Although microsomal fractions from renal cortex, inner stripe, and proximal papilla contained endosomes with H$^+$ATPase activity, microsomal fractions from distal papilla, 30 min after FITC-dextran infusion (Fig. 3 e), did not. When visualized in semi-thin sections (Fig. 1 c), endosomes from the distal papilla were still concentrated beneath the apical membrane of principal cells, similar to their location 15 min after FITC-dextran infusion. However, they were present at a lower density, suggesting that some FITC-dextran label was lost during the additional 15-min incubation period.

Passive Proton Permeability in Endosomes

Passive proton permeability ("proton leak") is conductive proton transport that is not coupled directly to other ions or solutes, and is independent of ATP (41). Passive proton permeability in endosomes was measured to (a) show that the lack of ATP-dependent acidification in endosomes from distal papilla was not the result of a very high proton leak specific to these vesicles; and (b) examine whether the VP-sensitive water channel that is also present in these vesicles had a high proton conductance.

Passive proton permeability was measured in FITC-dextran–labeled endosomes from the time course of endosome acidification in response to a 1.5-pH U inwardly directed proton gradient (pH$_{in}$ = 7.5, pH$_{out}$ = 6.0) (Fig. 4). A two-point pH calibration was performed in every experiment by addition of nigericin which caused rapid pH equilibration (see Materials and Methods). In endosomes from kidney cortex, the initial rate of pH decrease was 0.012 ± 0.002 pH U/s (+ VP, n = 3) and 0.014 ± 0.002 pH U/s (− VP). These values were converted to permeability coefficients (see Table II) by use of the intravesicular buffer capacity and the fluorescence vs. pH calibration relation. In endosomes from kidney papilla, the initial rate of pH decrease was 0.023 ± 0.004 pH U/s (+ VP) and 0.019 ± 0.006 pH U/s (− VP). Table II shows that VP pretreatment has minimal influence on the proton permeability coefficient in endosomes from cortex and papilla. In addition, the proton permeability coefficients of papillary endosomes are not sufficiently greater than that of cortical endosomes to account for the lack of ATP-dependent acidification in endosomes from distal papilla.

Water Permeability of Endosomes

To demonstrate that microsomes prepared from the distal papilla (which do not acidify) contained those endosomes that internalize water channels in response to VP, the osmotic water permeability (P$_f$) of endosomes labeled with 6-CF was measured by fluorescence quenching in response to an inwardly directed 100-mOsM sucrose gradient (Fig. 5 and Table II) (32, 46). Similar to our previous results (43), microsomal fractions from renal cortex contained two populations of endosomes; one with high P$_f$, characteristic of channel-mediated water transport, and one with low P$_f$, characteristic of water transport by lipid diffusion. The relative size of the population with high P$_f$ (fractional fast component) is indicated by the fraction of total decrease in fluorescence due to rapid fluorescence quenching. Microsomal fractions from renal cortex of rats treated or not treated with VP contained endosomes with water channels in their

Table I. Active Proton Transport in Endocytic Vesicles

	15 min after infusion		30 min after infusion	
	dpH/dt	pH$_{min}$	dpH/dt	pH$_{min}$
	pHU/s		pHU/s	
Distal papilla				
− VP	0.002 ± 0.004	7.50 ± 0.01	0.002 ± 0.004	7.48 ± 0.04
+ VP	0.003 ± 0.005	7.49 ± 0.01	0.004 ± 0.008	7.47 ± 0.01
Proximal papilla				
− VP	0.08 ± 0.01	7.32 ± 0.07	0.09 ± 0.03	7.24 ± 0.08
+ VP	0.12 ± 0.01	7.29 ± 0.08	0.15 ± 0.02	7.14 ± 0.02
Inner stripe				
− VP	0.07 ± 0.004	7.20 ± 0.02	0.12 ± 0.04	6.89 ± 0.02
+ VP	0.10 ± 0.01	7.10 ± 0.03	0.09 ± 0.01	7.07 ± 0.04
Cortex				
− VP	0.25 ± 0.08	5.87 ± 0.87	0.33 ± 0.03	6.30 ± 0.07
+ VP	0.18 ± 0.05	5.8 ± 0.56	0.32 ± 0.05	6.33 ± 0.17

Mean ± SD of 3–12 separate experiments.

limiting membrane (Table II). Microsomal fractions from inner stripe and proximal or distal papilla, however, contained endosomes with water channels only when rats were treated with VP (Fig. 5 and Table II). Though a population of endosomes from principal cells stimulated with VP contained water channels in their limiting membrane, these endosomes did not demonstrate ATP-dependent acidification, (Tables I and II).

Fluorescence Imaging Microscopy

The fraction of endosomes present in crude microsomal preparations was determined by the nonspecific absorption of microsomes to poly-l-lysine-coated coverslips. For these experiments, endosomes were first loaded in vivo with rhodamine-dextran instead of FITC-dextran (see Materials and Methods). Then, the entire population of isolated vesicles was labeled in vitro by incubation with 6-CF. Endosomes, now labeled with both rhodamine and fluorescein, could be distinguished from nonendocytic vesicles, labeled with fluorescein alone, by fluorescence imaging microscopy (Fig. 6). In a similar manner, the fraction of endosomes containing proton pumps, in corresponding microsomal preparations, was determined by the specific immunoabsorption of microsomes to coverslips coated with mAbs against the bovine vacuolar proton pump.

The results of these experiments are summarized in Table III. Endosomes account for ∼25% of the vesicles present in crude microsomal fractions from the cortex whether treated or not with VP. In contrast, endosomes account for a smaller fraction of the vesicles from the papilla (9–14%) and the fractional component was greater in rats treated with VP. This is consistent with morphological data showing that VP enhances the endocytic uptake of fluid phase markers in principal cells (9).

When microsomal preparations were incubated with coverslips coated with antibodies against the vacuolar proton pump, the fractional component of cortical endosomes were enriched by 1.5-fold. In contrast, the fractional component of papillary endosomes was significantly depleted by two to threefold. The results are consistent with biophysical data

which shows that apical endosomes from principal cells do not appear to contain a functional ATP-dependent proton pump.

Immunocytochemistry with LGP120

To demonstrate the relationship between lysosomal vesicles and endosomes in principal cells, we immunostained frozen semi-thin sections of distal papilla from rats treated with FITC-dextran and VP (15 min) with an antibody against the lysosomal membrane glycoprotein, LGP120, followed by rhodamine-labeled secondary antibody. Principal cells contained LGP120/rhodamine-labeled structures in the basal and lateral regions of the cell, around the nucleus (Fig. 7 b). LGP120-labeled structures were rarely found in subapical regions of the same cells where FITC-labeled endosomes were concentrated (Fig. 7 a), although a small amount of overlap could be detected in some areas. Because LGP120 may also stain late endosomes in some cells (19, 22), these results indicate that in principal cells, the bulk of endocytosed FITC-dextran remains in an early endosomal compartment. In contrast, LGP120 clearly stained a population of apical endosomes with entrapped FITC-dextran present in proximal tubule epithelia from the same kidney. A few larger lysosome-like structures that contained FITC-dextran were also stained with LGP 120 (Fig. 7, c and d). These results demonstrate that, in the collecting duct principal cell, most of the FITC-labeled endosomes do not contain the lysosomal glycoprotein, LGP120 at the time points examined.

Discussion

Principal cells of the renal collecting duct respond rapidly to VP stimulation by increasing the water permeability of their apical plasma membrane. The cellular mechanism which regulates this process is thought to involve exo- and endocytic trafficking of "water channels" between a pool of specialized cytoplasmic vesicles and the apical cell surface (4, 9, 20, 27, 42, 45). Using freeze-fracture EM and HRP as a tracer of endocytosis, we have previously shown that VP-induced clusters of intramembranous particles, which
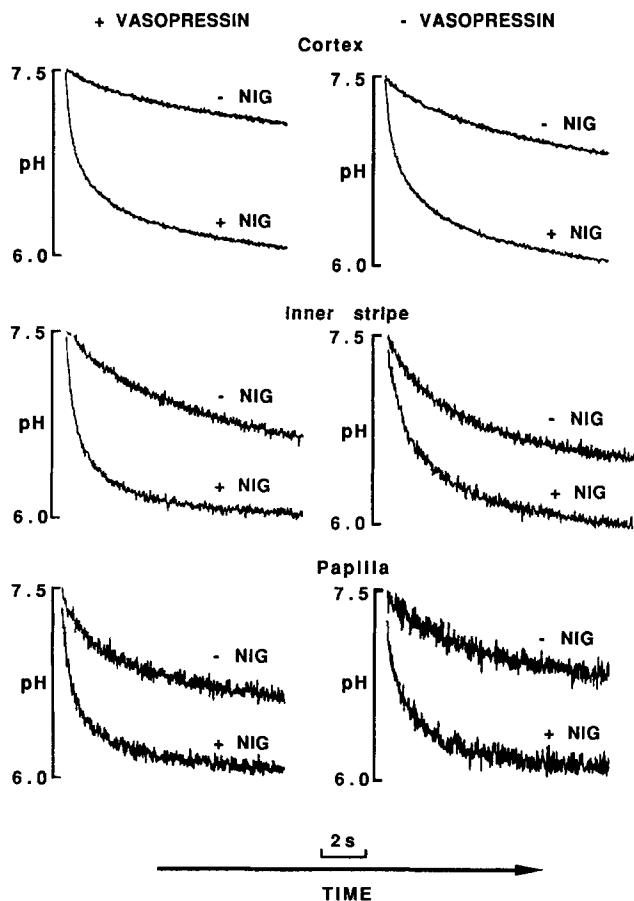
+ VASOPRESSIN   **- VASOPRESSIN**

Cortex

Inner stripe

Papilla

2 s

TIME

Figure 4. Passive proton permeability in endosomes from the cortex, inner stripe, and papilla (proximal and distal combined) of Brattleboro rats treated and not treated with VP. Endosomes labeled with FITC dextran in buffer B were subjected to a 1.5-pH U inwardly directed proton gradient (pH$_{in}$ = 7.5, pH$_{out}$ = 6.0) at 21°C. +*NIG* indicates that 5 μM nigericin was present in the endosome suspension. Curves from the cortex, inner stripe, and papilla were individually normalized to the same pH scale. When the curves were normalized per mg total membrane protein, signal amplitudes for vesicles from the cortex and inner stripe of untreated rats were identical to those from the same kidney regions of treated rats. The signal amplitude for vesicles from the papilla of untreated rats, however, was only 70.2% of that for vesicles from the papilla of rats treated with VP. Proton permeability coefficients are given in the text and in Table II.

Cortex

Proximal papilla

Distal papilla

Relative fluorescence

Time

Figure 5. Osmotic water permeability in endosomes from the cortex, proximal papilla, and distal papilla of Brattleboro rats treated and not treated with VP. Endosomes labeled with 6-CF in buffer A were subjected to a 100-mosM inwardly directed sucrose gradient causing osmotic water efflux, endosome shrinkage, and instantaneous 6-CF self-quenching. Experiments were carried out at 21°C. Curves labeled +VP and −VP for individual kidney segments were normalized to milligrams of total membrane protein. Data are shown using two different time scales to facilitate comparison between +VP and −VP curves. Curves on the shorter time scale were fitted to single (−*VP*) or biexponential (+*VP*) functions (thin line). Fitted P$_f$ values are given in Table II.

are believed to represent water channels, are localized in and are internalized by clathrin-coated pits on apical membranes of principal cells (5, 9). By making use of the self-quenching properties of entrapped fluoresceins to measure endosome water permeability, we then demonstrated directly that principal cells endocytose functional water channels from their apical membrane in response to VP, and that the presence of water channels in the limiting membrane of these endosomes is correlated with the antidiuretic state of the rat before kidney removal (43, Lencer et al., manuscript submitted for publication). In addition, purified clathrin-coated vesicles from bovine kidney cortex and medulla contain functional water channels, whereas those from brain do not (44). While it is now clear from these studies and from work on
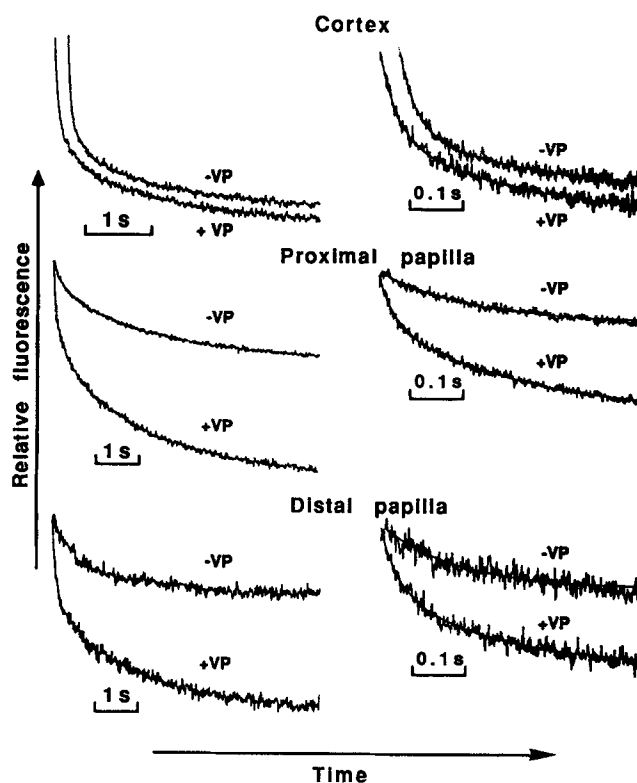
isolated perfused collecting tubules (36) that water channels are internalized from the apical plasma membrane of principal cells by clathrin-mediated endocytosis, subsequent steps in the processing of the internalized channels are undefined.

In this report, we examined ATP-dependent proton transport in endocytic vesicles which contain the VP-sensitive water channel, and found that these endosomes did not contain a functional ATP-dependent proton pump and were not immunoabsorbed with antiproton pump antibodies. Furthermore, the bulk of internalized FITC-dextran in collecting duct principal cells was present in structures that were distinct from those that labeled with antibodies against the lysosomal glycoprotein LGP120. These data are consistent with our previous studies on the immunolocalization of proton pumps in the kidney which failed to detect antigenic sites in principal cell endosomes, whereas apical vesicles in proximal tubules, intercalated cells, and cells of the distal convoluted tubule and thick ascending limbs of Henle were labeled (8). These data show that endosomes involved in trafficking the VP-sensitive water channel do not acidify and

Table II. Osmotic Water and Passive Proton Permeability of Endocytic Vesicles

	P_f*	Fractional fast component	P_{H+}	Relative H+ATPase	
				15 min	30 min
	cm/s		cm/s		
Distal papilla					
− VP	not present	not present	− − −	0.00 ± 0.01	0.02 ± 0.03
+ VP	0.038 ± 0.004	0.42 ± 0.05	− − −	0.01 ± 0.01	0.03 ± 0.01
Proximal papilla					
− VP	not present	not present	0.019 ± 0.006‡	0.17 ± 0.06	0.26 ± 0.03
+ VP	0.040 ± 0.005	0.35 ± 0.03	0.023 ± 0.004‡	0.20 ± 0.07	0.31 ± 0.04
Inner stripe					
− VP	not present	not present	0.023 ± 0.005	0.27 ± 0.01	0.51 ± 0.01
+ VP	0.043 ± 0.005	0.11 ± 0.02	0.020 ± 0.003	0.36 ± 0.03	0.37 ± 0.03
Cortex					
− VP	0.045 ± 0.002	0.61 ± 0.04	0.014 ± 0.002	1.0 (standard)	1.0 ± 0.05
+ VP	0.046 ± 0.002	0.59 ± 0.03	0.012 ± 0.002	0.87 ± 0.02	0.97 ± 0.14

* Fast component.
‡ Combined proximal and distal papilla.

do not transfer appreciable amounts of FITC-dextran to lysosomes.

Localization of Endosomes in Principal Cells

The interpretation of our functional data depends on the ability to identify the cell types from which FITC-dextran–loaded endosomes originate. This problem was overcome in our studies by isolating vesicles from different kidney regions, in which the epithelial cell population of the collecting duct is either heterogeneous (inner stripe and proximal papilla) or homogeneous (distal papilla). In addition, morphological studies enabled us to trace the cellular uptake of FITC-dextran in all kidney regions.

In the distal papilla, fluorescein-labeled endosomes were located close to the apical membrane of principal cells. No other cell type took up detectable amounts of FITC-dextran indicating that, in the biophysical assays, the overwhelming majority of fluorescence originated from the apical endocytic compartment of this cell type. In contrast, intercalated cells that are present alongside principal cells in tissue from the proximal papilla and inner stripe, but not the distal papilla (7, 11), took up large amounts of FITC-dextran and probably accounted for much of the ATP-dependent acidification in microsomal fractions from these regions of the kidney. Intercalated cells are known to cycle a vacuolar proton-pumping ATPase between intracellular vesicles and the plasma membrane (4, 6, 24, 30, 31), and ATP-driven acidification progressively increased in microsomal fractions from proximal papilla and inner stripe as the density of intercalated cells in these regions of the kidney increased. Similarly,
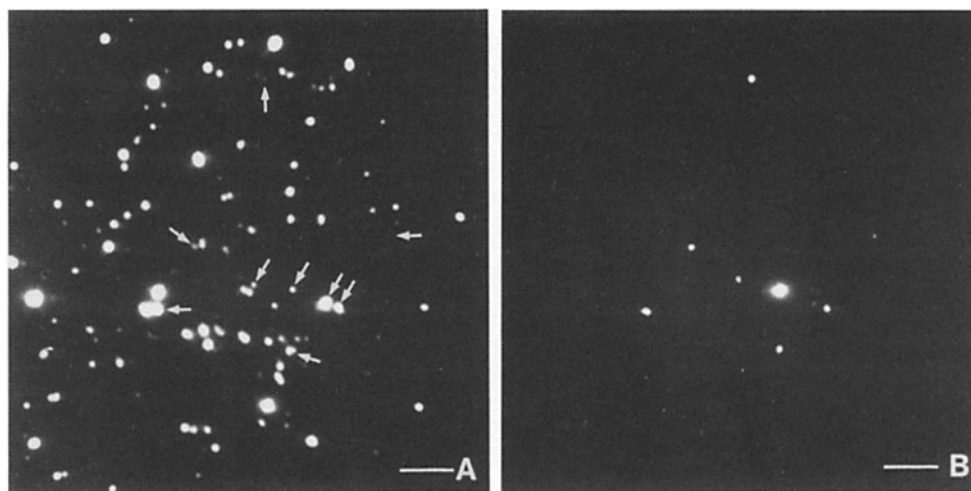

Figure 6. Fluorescence imaging microscopy of microsomes from the papilla of a Brattleboro rat treated with VP. For these experiments, endosomes were first loaded in vivo with rhodamine-dextran instead of fluorescein-dextran. Then, the entire population of isolated vesicles, endosomes, and nonendocytic vesicles, was labeled in vitro by incubation with 6-CF. Endosomes, now labeled with both rhodamine and fluorescein, could be distinguished from nonendocytic vesicles, labeled with fluorescein alone by fluorescence imaging microscopy. The fraction of endosomes present in microsomal preparations was determined by nonspecific absorption of microsomes to poly-l-lysine–coated coverslips. Fluorescein-labeled vesicles were visualized by exciting at 490 nm (A). Rhodamine-labeled endosomes in the same field were visualized by exciting at 560 nm (B). Each rhodamine-labeled endosome corresponds exactly to a fluorescein-labeled vesicle marked here with arrows. The fraction of endosomes containing proton pumps in corresponding microsomal preparations was determined by the specific immunoabsorption of microsomes to coverslips coated with mAbs against the bovine vacuolar proton pump. Bars, 5 μm.

Table III. Fractional Component of Endosomes in Microsomal Fractions

	Polylysine-coated coverslips	Anti-H$^+$ATPase antibody-coated coverslips
Cortex (+VP)	0.24 (n = 3,210)	0.39 (n = 387)
Cortex (−VP)	0.25 (n = 2,605)	0.34 (n = 648)
Papilla (+VP)	0.14 (n = 1,873)	0.04 (n = 945)
Papilla (−VP)	0.09 (n = 1,607)	0.05 (n = 668)

the presence of fluorescein-labeled endosomes from intercalated cells causes the fractional component of endosomes with water channels to decrease in microsomal fractions from proximal papilla and inner stripe. In VP-treated rats, the fractional component of endosomes with water channels was highest in distal papilla (0.42) and progressively decreased in proximal papilla (0.35) and inner stripe (0.11) as the number of intercalated cells containing endosomes without water channels increased. In the inner stripe, cells of the thick
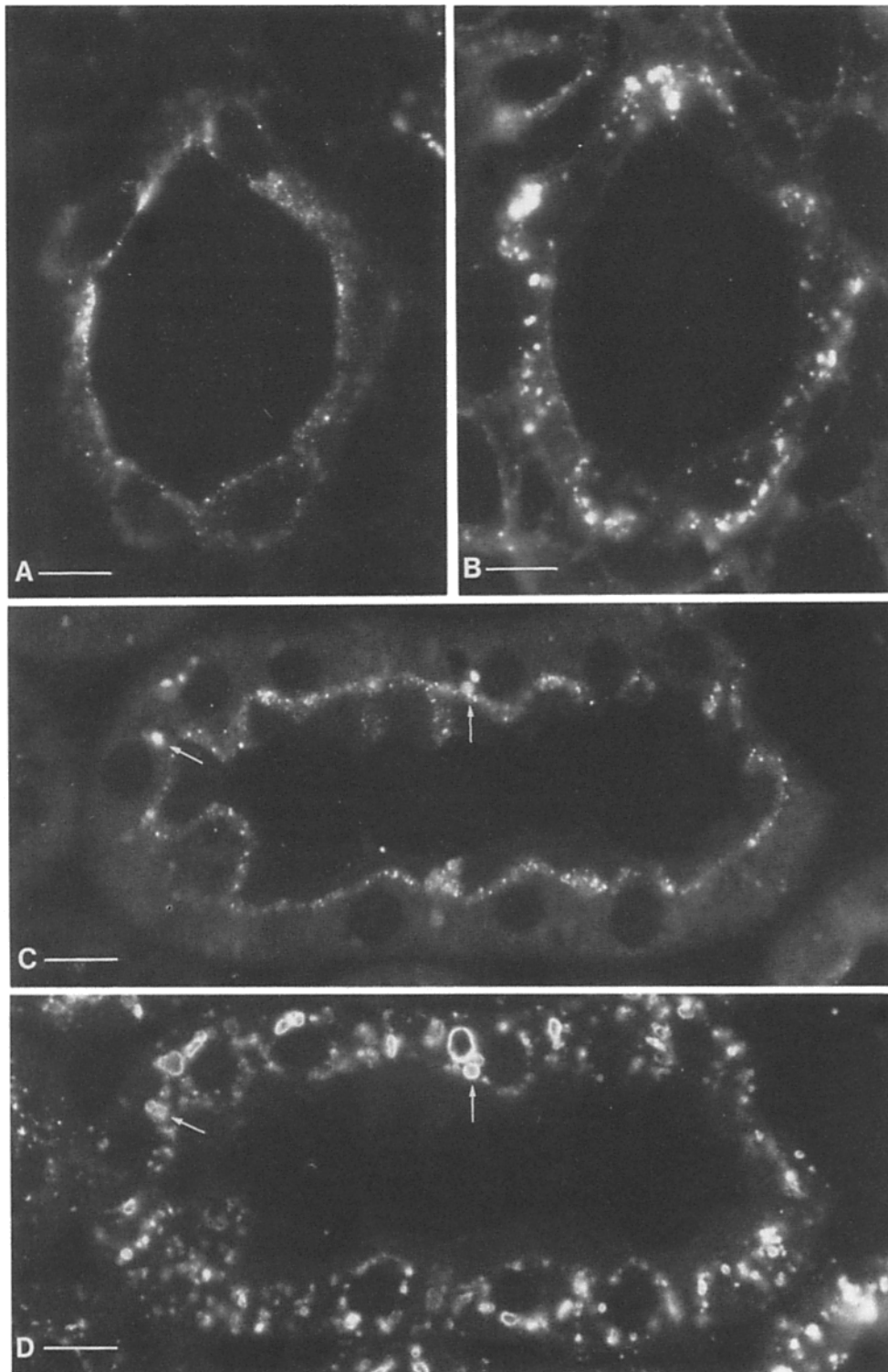

Figure 7. Fluorescent micrographs of a collecting duct from the distal papilla (*A* and *B*) and proximal tubule from the cortex (*C* and *D*) of a Brattleboro rat 15 min after infusion of FITC dextran and VP. The sections were also immunostained with antibodies against the lysosomal membrane glycoprotein LGP120. *A* shows that FITC-labeled endosomes, visualized by exciting at 490 nm, were concentrated at the apical pole of principal cells. These labeled endosomes did not colocalize with structures from the same cell that stained with LGP120 and rhodamine-labeled secondary antibody, visualized by exciting at 560 nm (*B*). In proximal tubule epithelia, some FITC-labeled endosomes (*C*, *arrows*) did colocalize with structures that stained with LGP120 (*D*, *arrows*). Bars, 10 μm.

ascending limb of Henle also internalized FITC-dextran and contributed to the population of endosomes without water channels in this region of the kidney. This tubule segment is always impermeable to water, but endosomes from the thick ascending limb do contain a proton-pumping ATPase that is detectable by immunocytochemistry (8).

Proton Transport in Endosomes Containing Water Channels

Whereas acidification due to a proton-pumping ATPase could be demonstrated in endosomes from proximal papilla, inner stripe, and cortex, endosomes from the distal papilla did not acidify in response to ATP. VP treatment caused principal cells to internalize water channels and enhance their rate of endocytosis, as previously described (9) but had no effect on the acidification of these vesicles. We could not detect acidification of the FITC-dextran containing endosomes from rats treated or not treated with VP either 15 or 30 min after FITC-dextran infusion. This indicates that the overwhelming majority of apical endosomes in principal cells did not progressively acquire functional proton pumps over time as found, for example, in CHO cells (29). The finding that passive proton transport (P_H) was similar in endosomes from the papilla, the inner stripe, and cortex shows that a high rate of proton leak across the limiting membrane of endosomes from the distal papilla did not account for the absence of detectable ATP-driven proton transport in these vesicles.

Indirect measurements of proton transport on intact toad urinary bladder in vitro suggested that water channels in toad bladder granular cells may also conduct protons (17). These data suggest that endosomes containing water channels should have a greater passive permeability to protons than endosomes without water channels, i.e., those from rats not treated with VP. In our studies, however, VP had no significant effect on passive proton transport in FITC-labeled endosomes from any region of the kidney, including the distal papilla. Similar findings from studies on P_H in FITC-labeled endosomes from toad bladder were recently reported (33) and red blood cells, which contain water channels in their limiting membrane, also have a very low proton conductance (23). Furthermore, we have shown recently that water channels and proton pumps coexist in the same endosomes isolated from the proximal tubule of rabbit cortex (46). The water permeability of these cortical endosomes was as high as that found in endosomes isolated from the papilla after treatment with VP but this did not prevent their acidification. Therefore, proximal tubule endosomes are able to demonstrate significant lumenal acidification despite the presence of water channels in their limiting membrane. Because our present data indicate that the presence of water channels in principal cell endosomes does not significantly increase passive proton permeability, the mechanism by which VP induces an increase in transepithelial proton conductance of the toad bladder remains to be determined.

Immunoabsorption and Immunocytochemistry

The presence of nonendocytic (i.e., unlabeled) vesicles capable of ATP-dependent acidification in microsomal fractions from distal papilla was demonstrated by the depletion of endocytic (i.e., labeled) vesicles on glass coverslips coated with antibodies against the bovine vacuolar H$^+$ATPase. Vesicles from the papilla were adherent to antibody-coated coverslips, but the fractional component of RITC-labeled endosomes in the adherent vesicles was reduced compared to that found when polylysine-coated coverslips were used. Since cell types other than principal cells in the distal papilla contribute unlabeled vesicles to the microsomal fractions, the depletion of endosomes on anti-H$^+$ATPase-coated coverslips may be due to the specific adherence of vesicles from other cell types. However, the fact that the lysosomal membrane glycoprotein LGP 120 was identified by immunocytochemistry on structures in principal cells strongly implies that these cells contain a functional lysosomal degradative pathway.

Proton Pumps in Clathrin-coated Pits and Vesicles

Because water channels are internalized by a clathrin-mediated mechanism (5, 9, 36), our results indicate that at least in principal cells, clathrin-coated pits derived from the apical plasma membrane, and their progeny, coated vesicles, do not contain functional proton pumps. While a proton-pumping ATPase can be readily detected on bulk coated vesicle preparations isolated from different sources (35), it is not known whether the H$^+$ATPase is present both in coated vesicles that are involved in the endocytic pathway and in those that participate in intracellular trafficking, for example, at the step of protein exit from the Golgi apparatus. A previous study has reported that coated vesicles in the endocytic pathway do not acidify their lumen (Fuchs, R., A. Ellinger, M. Pavelka, M. Peterlik, and I. Mellman. 1987. *J. Cell Biol.* 105:91a.) and studies immunolocalizing the weak base DAMP, a morphological marker of acidification, have revealed heterogeneity of labeling of coated vesicles in fibroblasts (1).

Trafficking of Water Channels

Both polarized and nonpolarized eukaryotic cells have an acidic endosomal compartment (15, 26, 28, 29, 37). Fluid phase markers of endocytosis, such as FITC-dextran, are readily transferred from early endosomes to lysosomes in other cell types, including macrophages (28) and fibroblasts (37, 39). However, the trafficking of internalized water channels as well as FITC-dextran into an acidic prelysosomal compartment in principal cells seems to be absent or reduced. Recent studies on cultured Madin-Darby kidney cells show that 90% of apical endosomes are either recycled to the apical membrane or undergo transcytosis to the basolateral membrane without entering a late endosomal compartment (2). In addition, several membrane receptors are known to recycle to the cell surface from early endosomes shortly after endocytosis. For example, internalized transferrin receptors rapidly recycle to the basolateral membrane after endocytosis with >99% efficiency (14). IgA-receptor complexes that reach the apical surface of Madin-Darby kidney cells are repetitively endocytosed and rapidly recycled until the receptor is clipped and dimeric sIgA is released (3). These receptors appear trapped in their respective apical or basolateral plasma membranes by an endo- and exocytotic process which may account for the polarity of their distribution within the cell (3). The transferrin receptor, however, is known to cycle from the basolateral membrane through an acidic compartment (40). In contrast, our data suggest that the principal cell contains a similar specialized apical endo-

cytic compartment which functions primarily to recycle apical membrane components but which does not acidify. The regulated membrane traffic that moves water channels through this nonacidifying endocytic compartment in principal cells appears to be part of a novel endocytic pathway that plays a fundamental role in the regulation of water reabsorption by the mammalian kidney.

References

1. Anderson, R. G. W., J. R. Falck, J. L. Goldstein, and M. S. Brown. 1984. Visualization of acidic organelles in intact cells by electron microscopy. *Proc. Natl. Acad. Sci. USA.* 81:4838–4842.
2. Bomsel, M., K. Prydz, R. G. Parton, J. Gruenberg, and K. Simons. 1989. Endocytosis in filter-grown Madin-Darby canine kidney cells. *J. Cell Biol.* 109:3243–3258.
3. Breitfield, P. P., J. M. Harris, and K. Mostov. 1989. Postendocytic sorting of the ligand for the polymeric immunoglobulin receptor in Madin-Darby canine kidney cells. *J. Cell Biol.* 109:475–476.
4. Brown, D. 1989. Membrane recycling and epithelial cell function. *Am. J. Physiol.* 256:F1–F12.
5. Brown, D., and L. Orci. 1983. Vasopressin stimulates the formation of coated pits in rat kidney collecting ducts. *Nature (Lond.).* 302:253–255.
6. Brown, D., S. Gluck, and J. Hartwig. 1987. Structure of the novel membrane-coating material in proton-secreting epithelial cells and identification as an H⁺ATPase. *J. Cell Biol.* 105:1637–1648.
7. Brown, D., S. Hirsch, and S. Gluck. 1988. An H⁺ATPase is present in opposite plasma membrane domains in subpopulations of kidney epithelial cells. *Nature (Lond.).* 331:622–624.
8. Brown, D., S. Hirsch, and S. Gluck. 1988. Localization of a proton-pumping ATPase in rat kidney. *J. Clin. Invest.* 82:2114–2126.
9. Brown, D., P. Weyer, and L. Orci. 1988. Vasopressin stimulates endocytosis in kidney collecting duct epithelial cells. *Eur. J. Cell Biol.* 46:336–340.
10. Chen, P. Y., D. Pearce, and A. S. Verkman. 1988. Membrane water and solute permeability determined quantitatively by self-quenching of an entrapped fluoreophore. *Biochemistry.* 27:5713–5718.
11. Clapp, W. L., K. M. Madsen, J. W. Verlander, and C. C. Tisher. 1987. Intercalated cells of the rat inner medullary collecting duct. *Kidney Int.* 31:1080–1087.
12. Forgac, M. 1989. Structure and function of vacuolar class of ATP-driven proton pumps. *Physiol. Rev.* 69:765–795.
13. Deleted in proof.
14. Fuller, S. D., and K. Simons. 1986. Transferrin receptor polarity and recycling accuracy in "tight" and "leaky" strains of Madin-Darby canine kidney cells. *J. Cell Biol.* 103:1767–1779.
15. Galloway, C. J., G. E. Dean, M. Marsh, G. Rudnick, and I. Mellman. 1983. Acidification of macrophage and fibroblast endocytic vesicles in vitro. *Proc. Natl. Acad. Sci. USA.* 80:3334–3338.
16. Giloh, H., and S. W. Sedat. 1982. Fluorescence microscopy: reduced photobleaching of rhodamine and fluorescein protein conjugates by n-propyl-gallate. *Science (Wash. DC).* 217:1252–1255.
17. Gluck, S., and Q. Al-Awqati. 1980. Vasopressin increases water permeability by inducing pores. *Nature (Lond.).* 284:631–632.
18. Gluck, S., and J. Caldwell. 1987. Immunoaffinity purification and characterization of H⁺ATPase from bovine kidney. *J. Biol. Chem.* 262:15780–15789.
19. Griffiths, G., B. Hoflack, K. Simons, I. Mellman, and S. Kornfeld. 1988. The mannose-6-phosphate receptor and the biogenesis of lysosomes. *Cell.* 52:329–341.
20. Handler, J. S. 1988. Antidiuretic hormone moves membranes. *Am. J. Physiol.* 235:F375–F382.
21. Lencer, W. I., P. Weyer, A. S. Verkman, D. A. Ausiello, and D. Brown. 1990. FITC-dextran as a probe for endosome function and localization in the kidney. *Am. J. Physiol.* 258:C309–C317.
22. Lewis, V., S. A. Green, M. Marsh, P. Vihko, A. Helenius, and I. Mellman. 1985. Glycoproteins of the lysosomal membrane. *J. Cell Biol.* 100:1839–1847.
23. Macey, R. I. 1984. Transport of water and urea in red blood cells. *Am. J. Physiol.* 246:C195–C203.
24. Madsen, K. M., and C. C. Tisher. 1986. Structure-function relationships along the distal nephron. *Am. J. Physiol.* 250:F1–F15.
25. McLean, I. W., and P. F. Nakane. 1974. Periodate-lysine paraformaldehyde fixative: a new fixative for immunoelectron microscopy. *J. Histochem. Cytochem.* 22:1077–1083.
26. Mellman, I., R. Fuchs, and A. Helenius. 1986. Acidification of the endocytic and exocytic pathways. *Annu. Rev. Biochem.* 55:663–700.
27. Muller, J., W. A. Kachadorian, and V. A. DiScala. 1980. Evidence that ADH-stimulated intramembrane particle aggregates are transferred from cytoplasmic to luminal membranes in toad bladder epithelial cells. *J. Cell Biol.* 85:83–95.
28. Ohkuma, S., Y. Moriyama, and T. Takano. 1982. Identification and characterization of a proton pump on lysosomes by fluorescein isothiocyanate-dextran fluorescence. *Proc. Natl. Acad. Sci. USA.* 79:2754–2762.
29. Schmid, S. L., R. Fuchs, P. Male, and I. Mellman. 1988. Two distinct subpopulations of endosomes involved in membrane recycling and transport to lysosomes. *Cell.* 52:73–83.
30. Schwartz, G. J., and Q. Al-Awqati. 1985. Carbon dioxide causes exocytosis of vesicles containing H⁺ pumps in isolated perfused proximal and collecting tubules. *J. Clin. Invest.* 75:1638–1644.
31. Schwartz, G. J., J. Barasch, and Q. Al-Awqati. 1985. Plasticity of functional epithelial polarity. *Nature (Lond.).* 318:368–371.
32. Shi, L.-B., and A. S. Verkman. 1989. Very high water permeability in vasopressin-dependent endocytic vesicles in toad urinary bladder. *J. Gen. Physiol.* 94:1101–1105.
33. Shi, L.-B., D. Brown, and A. S. Verkman. 1990. Water, proton and urea transport in toad bladder endosomes which contain the vasopressin-sensitive water channel. *J. Gen. Physiol.* In press.
34. Sklar, L. A., Z. G. Oades, A. J. Jesaitis, R. G. Painter, and C. G. Cochrane. 1981. Fluoresceinated chemotactic peptide and high-affinity antifluorescein antibody as a probe for temporal characteristics of neutrophil stimulation. *Proc. Natl. Acad. Sci. USA.* 78:7540–7544.
35. Stone, D. 1988. Proton-translocating ATPases: issues in structure and function. *Kidney Int.* 33:767–774.
36. Strange, K., M. C. Willingham, J. S. Handler, and H. W. Harris Jr. 1988. Apical membrane endocytosis via coated pits is stimulated by removal of antidiuretic hormone from isolated, perfused rabbit cortical collecting tubule. *J. Membr. Biol.* 103:17–28.
37. Tyco, B., and F. R. Maxfield. 1982. Rapid acidification of endocytic vesicles containing a₂ macroglobulin. *Cell.* 28:643–651.
38. Valtin, H. 1982. The discovery of the Brattleboro rat, recommended nomenclature, and the question of proper controls. *Ann. NY Acad. Sci.* 394:1–9.
39. Van Deurs, B., C. Ropke, and N. Thorball. 1984. Kinetics of pinocytosis studied by flow cytometry. *Eur. J. Cell Biol.* 34:96–102.
40. Van Renswoude, J., J. B. Bridges, J. B. Harford, and R. Klausner. 1982. Receptor-mediated endocytosis of transferrin and the uptake of Fe in K562 cells: identification of a nonlysosomal acidic compartment. *Proc. Natl. Acad. Sci. USA.* 79:6186–6190.
41. Verkman, A. S. 1987. Passive H⁺/OH⁻ permeability in epithelial brush border membranes. *J. Bioenerg. Biomembr.* 19:481–493.
42. Verkman, A. S. 1989. Mechanisms and regulation of water permeability in renal epithelia. *Am. J. Physiol.* 257:C837–C850.
43. Verkman, A. S., W. I. Lencer, D. Brown, and D. A. Ausiello. 1988. Endosomes from kidney collecting tubule cells contain the vasopressin-sensitive water channel. *Nature (Lond.).* 333:268–269.
44. Verkman, A. S., P. Weyer, D. Brown, and D. A. Ausiello. 1989. Functional water channels are present in clathrin coated vesicles from bovine kidney but not from brain. *J. Biol. Chem.* 264:20608–20613.
45. Wade, J. B., D. L. Stetson, and S. A. Lewis. 1981. ADH action: evidence for a membrane shuttle mechanism. *Ann. NY Acad. Sci.* 372:106–117.
46. Ye, R., L. B. Shi, W. I. Lencer, and A. S. Verkman. 1989. Functional colocalization of water channels and proton pumps in endosomes from kidney proximal tubule. *J. Gen. Physiol.* 93:885–902.
47. Yurko, M., and S. Gluck. 1987. Production and characterization of a monoclonal antibody to vacuolar H⁺ATPase of renal epithelia. *J. Biol. Chem.* 262:15770–15779.